ber of fissions resulting from each of the three uranium nuclei and the weighted average mass numbers of the fissioning nuclei were calculated from the Γ_n/Γ_f ratios of Vandenbosch and Huizenga.[38] For fission of U^{235} and U^{238} with 14.6-MeV neutrons, the average numbers of neutrons emitted from fragments per fission were estimated from these values to be 3.74 and 3.40, respectively, giving curves II and III of Fig. 1. The average mass numbers of the fissioning nuclei are 235.2 and 238.0. The neutron-emission curve of Whetstone[39] for 14-MeV neutron fission of U^{235} is quite different in shape from the curves considered above and has much larger uncertainties, but it gives essentially the same values of ν in the mass regions of interest.

[38] R. Vandenbosch and J. R. Huizenga, in *Proceedings of the Second International Conference on the Peaceful Uses of Atomic Energy*, 1958 (United Nations, Geneva, 1958), Vol. 15, pp. 284–294.

[39] S. L. Whetstone, Phys. Rev. **133**, B613 (1964).

ACKNOWLEDGMENTS

The author wishes to thank Dr. G. A. Cowan and Dr. J. D. Knight for their interest and advice, Dr. A. C. Wahl for valuable discussions of the manuscript, Dr. A. E. Norris for making his thesis available prior to its publication, Dr. J. Mattauch for furnishing the Z_A values, J. Povelites for preparing the thin deposits of U^{233} and Pu^{239}, and the personnel at the Water-Boiler reactor and the Cockcroft-Walton accelerator.

PHYSICAL REVIEW VOLUME 137, NUMBER 4B 22 FEBRUARY 1965

Exact Multiple-Scattering Analysis of Low-Energy Elastic K^--d Scattering with Separable Potentials*

J. H. HETHERINGTON AND L. H. SCHICK
School of Physics, University of Minnesota, Minneapolis, Minnesota
(Received 2 October 1964)

A calculation of the K^--d low-energy elastic-scattering cross sections is carried out with the intent of determining the importance of multiple scatterings. Under the assumption that the two-body interactions are S-wave nonlocal separable potentials of the Yamaguchi form, an expression for the scattering amplitude in terms of a set of one-dimensional integral equations for each partial wave is derived. The derivation does not take into account Coulomb forces or the n-p and K^--$\bar{K}^0$ mass differences. A transformation from real to complex dummy variables that allows a rapid numerical computation of the solution to the integral equations for the scattering amplitude is presented and discussed. With the use of the Humphrey and Ross kaon-nucleon scattering lengths, the elastic angular distribution and cross section, as well as the total cross section, are calculated for incident kaon lab momenta of 105, 194, and 300 MeV/c. The results of the multiple-scattering calculation for the elastic cross section are two to three times smaller than the impulse approximation results throughout this momentum range. The multiple-scattering corrections to the impulse approximation for the total cross section are small ($\lesssim 10\%$) only at the largest momentum used.

I. INTRODUCTION

THE intent of this theoretical investigation is to determine the contribution of the multiple scattering terms in low-energy K^--deuteron elastic scattering. By multiple scattering (MS) terms we mean that part of the expansion of the K^--d t matrix beyond the sum of the free K^--n and K^--p t matrices. By low-energy we mean those center-of-mass energies which lie above the threshold for deuteron breakup and below about 70 MeV. Our attention will be focused for the most part on K^--d elastic scattering, but the formalism developed may be applied with varying degrees of modification to K^+-d, π-d, or N-d scattering (elastic or inelastic), or any scattering problem in which the forces are of short range and the target may be considered to be a two-particle composite.

* Work supported in part by the U. S. Atomic Energy Commission.

In the past two types of approximations have been applied to the MS series for scattering from deuterons. In the first of these the motion of the neutron and proton are treated adiabatically and the recoil of these particles when struck by the incident particle is neglected; i.e., the incident particle is considered to be scattered by two potentials a fixed distance apart, this distance being averaged according to the deuteron ground-state probability distribution after the scattering amplitude has been calculated. Here it is found that for several types of simplified two-particle t matrices the MS series for the scattering amplitude may be summed into a closed form. Such simplifications included nonlocal separable (NLS) t matrices,[1] zero-range t matrices,[2,3] and t matrices whose matrix elements off the energy shell,[1,4] or in all but one

[1] S. D. Drell and L. Verlet, Phys. Rev. **99**, 849 (1955).
[2] K. A. Brueckner, Phys. Rev. **89**, 834 (1953); **90**, 715 (1953).
[3] R. Chand, Ann. Phys. **22**, 438 (1963).
[4] T. B. Day, G. A. Snow, and J. Sucher, Nuovo Cimento **11**, 637 (1959); Phys. Rev. **119**, 1100 (1960).

angular-momentum channel,[1–4] vanished. The contribution of the MS terms calculated in this manner for K^--d scattering is not insignificant for incident kaon lab momenta up to 200 MeV/c.[4]

In the other type of approximation the MS series is truncated. The most violent such truncation is the impulse approximation in which only the single-scattering terms are retained.[5,6] Some calculations have been performed in which, in addition to the single-scattering terms, the double-scattering terms have been retained.[7,8] In these calculations simplified forms for the two-particle t matrices, such as those mentioned above, were used in order to make the expressions for the various cross sections amenable to numerical treatment.

We wish to investigate the importance of the MS terms when neither a truncation nor a fixed scatterers approximation is used. The assumption that we make in order to carry out this investigation is that the two-body potentials have a particularly simple form: They are assumed to be S-wave NLS potentials.

Our primary concern here is not to obtain agreement with experiment, but rather to test the validity of the truncation approximation with a particular form for the two-body potentials. The parameters in these two-body interactions are chosen to fit the low-energy experimental data, but mainly to insure that any general conclusions drawn from our results are applicable to the physical problem.

It should be noted that NLS potentials have been previously applied to similar problems by Mitra, who treated the triton binding energy[9] and neutron-deuteron scattering at zero energy.[10] Our work differs from Mitra's in that we work with the t matrix rather than the wavefunction and our discussion is not restricted to the case of identical particles—a case which is actually simpler than the one treated here. Most importantly, we calculate cross sections at energies above the threshold for deuteron breakup. In this energy region the numerical evaluation of the theoretical expressions is more complicated than it is at lower energies.

In Sec. II.A we derive the basic set of integral equations from which the scattering amplitude may be calculated. These equations are of the Faddeev-Lovelace type.[11,12] With the use of the assumption that each two-particle interaction is an S-wave NLS potential, they reduce to a set of one-dimensional equations for each partial wave. Explicit results are presented for the case of K^--d scattering with Yamaguchi potentials. Spin, isospin, the identity of the nucleons and charge exchange scatterings are taken into account, but Coulomb forces and the n-p and K^--$\bar{K}^0$ mass differences are neglected.

In Sec. II.B a method for solving the basic equations numerically at energies above the threshold for deuteron breakup is developed. At these energies the kernels of the integral equations in a momentum-space representation contain singularities at distances of the order of η, $\eta \to 0^+$ above the real axes: i.e., at distances η from the contours of integration. In the method presented we let all the momenta over which we integrate become complex and evaluate each integral on a contour in the complex momentum plane that lies relatively far away from all singularities of the integrand. Each integrand is thus made a fairly slowly varying function of its arguments, so that the solution to the integral equations, and hence the scattering amplitude, can be calculated numerically.

In Sec. III we introduce kaon-nucleon scattering amplitudes whose scattering lengths are adjusted to the results of Humphrey and Ross,[13] but whose ranges are chosen rather arbitrarily. The nucleon-nucleon potential parameters are those originally used by Yamaguchi.[14] Several plots illustrating the effects of the deformation of the integration contours are presented. Results for the K^--d angular distribution, elastic cross section and total cross section are presented for incident kaon lab momentum of 105, 194, and 300 MeV/c. These results, especially as they concern the validity of the single scattering and double scattering approximations, are discussed in detail. The dependence of the calculation on the K^--N parameters is briefly investigated.

A summary of the work is given in Sec. IV.

II. THE MULTIPLE-SCATTERING EQUATIONS

A. Derivation

We calculate the matrix element $\mathfrak{M}_{ab}$ for elastic K^--d scattering at a total energy E,

$$\mathfrak{M}_{ab}=\langle a|T|b\rangle. \tag{1}$$

The states $|a\rangle$, $|b\rangle$ are each a product of a spatial wave function and an isospin wave function.[15] The spatial wave function is a product of a bound-state wave function for the relative motion of the nucleons, a plane wave for the relative kaon-deuteron motion, and a plane wave for the motion of the center of mass of the whole system. The isospin wave function consists of an isospin

[5] For π-d calculations see S. Fernbach, T. Green, and K. Watson, Phys. Rev. **84**, 1084 (1951); R. M. Rockmore, *ibid.* **105**, 256 (1957); **113**, 1696 (1959).

[6] For K-d calculations see E. M. Ferreira, Phys. Rev. **115**, 1727 (1959); V. J. Stenger, W. E. Slater, D. H. Stork, H. K. Ticho, G. Goldhaber, and S. Goldhaber, *ibid.* **134**, B1111 (1964).

[7] A. Everett, Phys. Rev. **126**, 831 (1962).

[8] A. K. Bhatia and J. Sucher, Phys. Rev. **132**, 855 (1963).

[9] A. N. Mitra, Nucl. Phys. **32**, 529 (1962).

[10] A. N. Mitra and V. S. Bhasin, Phys. Rev. **131**, 1265 (1963).

[11] L. D. Faddeev, Zh. Eksperim. i Teor. Fiz. **39**, 1459 (1960) [English transl.: Soviet Phys.—JETP **12**, 1014 (1961)]; Dokl. Akad. Nauk **138**, 561 (1961) [English transl.: Soviet Phys.—Doklady **6**, 384 (1961); Dokl. Akad. Nauk **145**, 301 (1962) [English transl.: Soviet Phys.—Doklady **7**, 600 (1963)].

[12] C. Lovelace, Lectures at Edinburgh Summer School, in *Strong Interactions in High Energy Physics*, edited by R. G. Moorhouse (Plenum Press, New York, 1964); Phys. Rev. **135**, B1225 (1964).

[13] W. R. Humphrey and R. R. Ross, Phys. Rev. **127**, 1305 (1962).

[14] Y. Yamaguchi, Phys. Rev. **95**, 1628 (1954).

[15] We have not included any spin-flip mechanism in our calculation. The spin dependence of the wave function is therefore trivial and has been omitted.

singlet function for the nucleons coupled to the kaon isospin to form a state of total isospin $\frac{1}{2}$ and z component $-\frac{1}{2}$. The t matrix T is an energy-dependent operator, but, as for all such operators this energy dependence is suppressed.

We let particle 2 be kaon and particles 1 and 3 the nucleons. The operator T satisfies the Lippmann-Schwinger equation[16]

$$T=(V_1+V_3)+(V_1+V_3)G_2T, \tag{2}$$

where the Green's function G_2 is defined by

$$G_2=[E-K-V_2+i\eta]^{-1}, \quad \eta\to 0^+. \tag{3}$$

Here K is the total three-particle kinetic energy operator and V_i is the potential between particles j and k where $j\neq i$ and $k\neq i$.

As the first step in the analysis, we convert Eq. (2) into a set of coupled equations involving the two-particle t matrices rather than the potentials. The formal solution to Eq. (2) is

$$T=(V_1+V_3)[1-G_2(V_1+V_3)]^{-1}. \tag{4}$$

Using the identity

$$G_2=[1-GV_2]^{-1}G, \tag{5}$$

where G is the free three-particle Green's function

$$G=[E-K+i\eta]^{-1}, \tag{6}$$

we obtain after some straightforward operator algebra

$$T=\sum_{i,j\neq 2} T^{ij} \tag{7}$$

with

$$T^{ij}=V_i\delta_{i,j}+V_i[1-G\sum_{k=1}^{3}V_k]^{-1}GV_j, \quad i,j=1,2,3, \tag{8}$$

$\delta_{i,j}$ being a Kronecker delta. Equation (8) is the formal solution of

$$T^{ij}=V_i\delta_{i,j}+V_iG\sum_{k=1}^{3}T^{kj}. \tag{9}$$

Separating out from the sum on the right of Eq. (9) the term with $k=i$, combining it with the left-hand side, and multiplying the result by $[1-V_iG]^{-1}$, we obtain the desired set of coupled equations[17]

$$T^{ij}=t_i\delta_{i,j}+\sum_{k=1}^{3}t_i\hat{G}^{ik}T^{kj}, \quad i,j=1,2,3, \tag{10}$$

where

$$t_i=V_i[1-GV_i]^{-1}, \tag{11}$$

$$\hat{G}^{ik}=G(1-\delta_{i,k}). \tag{12}$$

[16] B. A. Lippmann and J. Schwinger, Phys. Rev. **79**, 469 (1950).

[17] These equations were originally given by Faddeev, see Ref. 11. The derivation has been included here for completeness. See also the work of Lovelace, Ref. 12.

The operator t_i is the t matrix for the two-body scattering of particles j and k ($i\neq j$, $i\neq k$) with particle i as a noninteracting spectator, the total energy of all three particles being E. The iteration of Eq. (10) gives the multiple-scattering series

$$T^{ij}=t_i\delta_{i,j}+t_i\hat{G}^{ij}t_j+t_i\hat{G}^{ik}t_k\hat{G}^{kj}t_j+\cdots, \tag{13}$$

for i, $j=1$, 2, or 3 and in the triple-scattering term $k\neq i$, $k\neq j$. This expression shows that T^{ij} is just that part of T in which the initial scattering takes place with particle j as the spectator, while in the final scattering particle i is the spectator.

Our next step is to take matrix elements of Eq. (10). This is most conveniently done in terms of the "natural" coordinate systems for the operators t_i. Since t_i is the t matrix for the scattering of particles j and k ($i\neq j$, $i\neq k$), the natural system in which to take momentum-space matrix elements of this operator includes the total momentum q_i and the relative momentum k_i of these two particles. For the third momentum vector in each system we take the total momentum P. In terms of the lab-system momenta p_i, p_j, p_k, of particles i, j, k, respectively,

$$\mathbf{P}=\mathbf{p}_i+\mathbf{p}_j+\mathbf{p}_k, \tag{14}$$

$$\mathbf{q}_i=\mathbf{p}_j+\mathbf{p}_k, \tag{15}$$

$$\mathbf{k}_i=(m_j\mathbf{p}_k-m_k\mathbf{p}_j)/\mathfrak{M}_i. \tag{16}$$

Here m_i is the mass of the ith particle, $\mathfrak{M}_i=m_j+m_k$, and ijk is a cyclic permutation of 123. In the ith natural momentum-space coordinate system we have a complete set of plane wave states $|\mathbf{P},\mathbf{q}_i,\mathbf{k}_i\rangle$.

The isospin coordinates can be treated in an analogous manner. The ith isospin basis set is labeled by the total isospin ρ, its z component ζ, and the total isospin of particles j and k ($i\neq j$, $i\neq k$) which we denote by I. (We denote the total isospin of particles i and k, $i\neq j$, $k\neq j$, by J and the total isospin of particles i and j, $i\neq k$, $j\neq k$, by K.) Combining this state with the ith natural momentum state we obtain the ith basis state

$$|\mathbf{P},\mathbf{q}_i,\mathbf{k}_i;\rho,\zeta,I\rangle\equiv|i\rangle.$$

Taking the matrix element of Eq. (10) between the state

$$|\mathbf{P}',\mathbf{q}_j',\mathbf{k}_j';\rho',\zeta',J'\rangle\equiv|j'\rangle$$

on the right and the state $\langle i|$ on the left, we have, after insertion of the complete set

$$|\mathbf{P}'',\mathbf{q}_k''\cdots\rangle\langle\mathbf{P}'',\mathbf{q}_k''\cdots|=|k''\rangle\langle k''|$$

between $\hat{G}^{ik}$ and T^{kj},

$$\langle i|T^{ij}|j'\rangle=\langle i|t_i|i'\rangle\delta_{i,j}+\sum_{n=1}^{3}\int d''k\langle i|t_i\hat{G}^{ik}|k''\rangle\langle k''|T^{kj}|j'\rangle, \tag{17}$$

where

$$\int d''k \equiv (2\pi)^{-9} \sum_{\rho''} \sum_{\zeta''} \sum_{K''} \int d\mathbf{P}'' d\mathbf{q}_k'' d\mathbf{k}_k''. \quad (18)$$

The kernel of Eq. (17) itself may be expanded as

$$\langle i|t_i\hat{G}^{ik}|k''\rangle = \int d'''i \langle i|t_i|i'''\rangle \langle i'''|\hat{G}^{ik}|k''\rangle. \quad (19)$$

In the two-body scattering described by $\langle i|t_i|i'\rangle$ the total momentum of the three-body system and the total momentum of the two scattering particles are conserved, as are the isospins ρ, ζ, and I. This matrix element has the form then

$$\langle i|t_i|i'\rangle = (2\pi)^6 \delta(\mathbf{P}-\mathbf{P}')\delta(\mathbf{q}_i-\mathbf{q}_i')\delta_{\rho,\rho'}\delta_{\zeta,\zeta'}\delta_{I,I'} \times \langle \mathbf{k}_i|t_i(\mathbf{q}_i,\mathbf{P};I)|\mathbf{k}_i'\rangle. \quad (20)$$

The matrix element $\langle \mathbf{k}_i|t_i(\mathbf{q}_i,\mathbf{P};I)|\mathbf{k}_i'\rangle$ is the isospin I amplitude for the scattering of particles j and k in their center-of-mass system from a state of relative momentum $\mathbf{k}_i'$ to a state of relative momentum $\mathbf{k}_i$. The energy at which this two-body scattering takes place is

$$E-(2m_i)^{-1}(\mathbf{P}-\mathbf{q}_i)^2-(2\mathfrak{M}_i)^{-1}q_i^2. \quad (21)$$

The matrix element $\langle i|\hat{G}^{ik}|k'\rangle$ may be obtained from the matrix element

$$\langle \mathbf{p}_1,\mathbf{p}_2,\mathbf{p}_3; X,Y,Z|\hat{G}^{ik}|\mathbf{p}_1',\mathbf{p}_2',\mathbf{p}_3'; X',Y',Z'\rangle,$$

where X, Y, Z are the z components of the isospin of particles 1, 2, and 3, respectively. From Eqs. (6) and (12) this latter matrix element is equal to

$$D^{-1}(\mathbf{p}_i,\mathbf{p}_j,\mathbf{p}_k)(1-\delta_{i,k})(2\pi)^9 \times \delta_{X,X'}\delta_{Y,Y'}\delta_{Z,Z'} \prod_{i=1}^{3} \delta(\mathbf{p}_i-\mathbf{p}_i'), \quad (22)$$

where

$$D(\mathbf{p}_i,\mathbf{p}_j,\mathbf{p}_k) = E-(2m_i)^{-1}p_i^2 - (2m_j)^{-1}p_j^2-(2m_k)^{-1}p_k^2+i\eta, \quad (23)$$

with i, j, k distinct. With the aid of Eqs. (14), (15), and (16) we may transform from the $\mathbf{p}_1$, $\mathbf{p}_2$, $\mathbf{p}_3$ coordinate system to the $\mathbf{P}$, $\mathbf{q}_i$, $\mathbf{k}_i$ system and from the $\mathbf{p}_1'$, $\mathbf{p}_2'$, $\mathbf{p}_3'$ system to the $\mathbf{P}'$, $\mathbf{q}_k'$, $\mathbf{k}_k'$ system. We can perform analogous transformations in isospin space. By use of all of these transformations we obtain

$$\langle i|\hat{G}^{ik}|k'\rangle = (2\pi)^9(1-\delta_{i,k})\delta(\mathbf{P}-\mathbf{P}')\delta_{\rho,\rho'}\delta_{\zeta,\zeta'}U^{ik}(I,K') \times D^{-1}(\mathbf{P}-\mathbf{q}_i,\ \mathbf{q}_i+\mathbf{q}_k'-\mathbf{P},\ \mathbf{P}'-\mathbf{q}_k')\delta_{ik}(,')\delta_{ki}(',), \quad (24)$$

where

$$\delta_{ik}(,') = \delta(\mathbf{P}-\mathbf{q}_i-(m_i/\mathfrak{M}_k)\mathbf{q}_k' \pm \mathbf{k}_k'), \quad \delta_{ki}(',) = \delta(-\mathbf{P}'+\mathbf{q}_k'+(m_k/\mathfrak{M}_i)\mathbf{q}_i \pm \mathbf{k}_i). \quad (25)$$

In the last two equations the upper (lower) signs are used if the numbers i, k are a cyclic (anticyclic) pair of the numbers 1, 2, 3. The matrix elements of the isospin space transformation from the kth to the ith natural system $U^{ik}(I,K')$ are given in Appendix A.

We now combine Eqs. (17) through (20) with Eqs. (24) and (25). In doing so we factor out the total-momentum conserving δ function and the Kronecker δ's which conserve total isospin and its z component. For convenience we continue the analysis in the zero-momentum frame of reference with our basis states now having the form $|\mathbf{q}_i,\mathbf{k}_i;I\rangle$. We obtain the set of coupled equations

$$\langle \mathbf{q}_i,\mathbf{k}_i;I|T^{ij}|\mathbf{q}_j',\mathbf{k}_j';J'\rangle = (2\pi)^3\delta(\mathbf{q}_i-\mathbf{q}_j')\langle \mathbf{k}_i|t_i(q_i,I)|\mathbf{k}_i'\rangle\delta_{i,j}\delta_{I,J'} + \sum_{k=1}^{3}(1-\delta_{i,k})\sum_{K''=0}^{1}\int (2\pi)^{-3}d\mathbf{q}_k'' D^{-1}(\mathbf{q}_i,\ \mathbf{q}_i+\mathbf{q}_k'',\ \mathbf{q}_k'')U^{ik}(I,K'') \times \langle \mathbf{k}_i|t_i(q_i,I)|\mp(m_k/\mathfrak{M}_i)\mathbf{q}_i\mp\mathbf{q}_k''\rangle\langle \mathbf{q}_k'',\ \mp\mathbf{q}_i\mp(m_i/\mathfrak{M}_k)\mathbf{q}_k''; K''|T^{kj}|\mathbf{q}_j',\mathbf{k}_j';J'\rangle, \quad (26)$$

where $t_i(q_i,I)\equiv t_i(\mathbf{q}_i,0;I)$.

Equation (26) is exact, but too complicated to be useful for numerical application. In order to proceed further, we make the simplifying assumption that all three two-body potentials are S-wave NLS potentials; i.e., in terms of isospin and configuration-space matrix elements

$$\langle \mathbf{r}_{jk};I|V_i|\mathbf{r}_{jk}';I'\rangle = \lambda_i(I)v_i(r_{jk},I)v_i(r_{jk}',I')\delta_{I,I'}, \quad (27)$$

where $\mathbf{r}_{jk}$ is the relative position of particles j and k, and $r_{jk}=|\mathbf{r}_{jk}|$. It follows that

$$\langle \mathbf{k}_i|t_i(q_i,I)|\mathbf{k}_i'\rangle = v_i(k_i,I)\tau_i(q_i,I)v_i(k_i',I), \quad (28)$$

where

$$v_i(k_i,I) = \int d\mathbf{r}_{jk} v_i(r_{jk},I)\exp[i\mathbf{k}_i\cdot\mathbf{r}_{jk}], \quad (29)$$

$$\tau_i(q_i,I) = \lambda_i(I)[1-\lambda_i(I)\gamma_i(q_i,I)]^{-1}, \quad (30)$$

$$\gamma_i(q_i,I) = \int \frac{d\mathbf{k}_i v_i^2(k_i,I)}{(2\pi)^3[E-(\mathfrak{M}/2m_i\mathfrak{M}_i)q_i^2-(k_i^2/2\mu_i)+i\eta]}, \quad (31)$$

$$\mathfrak{M}=m_1+m_2+m_3, \quad \mu_i=\mathfrak{M}_i^{-1}m_jm_k. \quad (32)$$

Although it is not at all necessary to the development of the analysis, we assume for convenience that each potential is of the Yamaguchi form[13]:

$$v_i(k_i,I)=[k_i^2+\beta_i^2(I)]^{-1}. \tag{33}$$

Using Eq. (28) in Eq. (26) we may factor out the dependence of the latter on k_i and k_j'. The kernel of the resulting set of six coupled equations depends only on the magnitudes and the relative angle of the momenta $\mathbf{q}_i$ and $\mathbf{q}_k''$. By manipulation[18] we reduce this set to a set of three coupled equations. A partial-wave analysis is then carried out leaving a set of three simultaneous integral equations in one dimension. By taking the range of the kaon-nucleon potentials to be isospin-independent[19] and combining these equations with Eq. (1), we obtain the following set of equations[20]:

$$\mathfrak{M}_{ab}=(2\pi)^3\delta(\mathbf{P}_a-\mathbf{P}_b)\delta_{\rho,\rho'}\delta_{\zeta,\zeta'}M_{ab}, \tag{34}$$

$$M_{ab}=\sum_l(2l+1)[\eta_l^{\mathrm{IA}}+\eta_l^{\mathrm{MS}}]P_l(\hat{q}_a\cdot\hat{q}_b), \tag{35}$$

$$\eta_l^{\mathrm{IA}}=\sum_\gamma\int_0^\infty\Phi_{l\gamma 2}(q,q_a)\tau^\gamma(q)\Phi_{l\gamma 2}(q,q_a)(2\pi)^{-2}q^2dq, \tag{36}$$

$$\eta_l^{\mathrm{MS}}=\sum_\alpha\sum_\beta\int_0^\infty\int_0^\infty\Phi_{l\alpha 2}(q,q_a)\tau^\alpha(q)R_{l\alpha\beta}(q,q')\tau^\beta(q')\times\Phi_{l\beta 2}(q',q_a)(2\pi)^{-4}q^2q'^2dqdq'. \tag{37}$$

In Eq. (34) ρ,ζ (ρ',ζ') are the total isospin and its z component in the final (initial) state, respectively. The vectors $-\mathbf{q}_a$ and $-\mathbf{q}_b$ are, respectively, the final and the initial kaon momentum in the zero total-momentum frame. The meaning of the rest of the notation used in Eqs. (34) and (35) is manifest.

The vector $\tau^\gamma(q)$ is given by

$$[\tau^\gamma(q)]=\begin{bmatrix}\tau_1(q,0)\\ \tau_2(q,0)\\ \tau_1(q,1)\end{bmatrix}.$$

For the lth partial wave the vector $\Phi_{l\gamma 2}(q,q_a)$ is given by

$$\Phi_{l\gamma 2}(q,q_a)=-\mathcal{Q}_l(Z_{\gamma 2},Z_{2\gamma},\bar{Z}_{2\gamma})\left(\frac{\mathfrak{M}_2^2\mathfrak{M}_\gamma}{8m_2m_\gamma^2}\right)\frac{N_2C_\gamma}{(qq_a)^3}, \tag{38}$$

where

$$\mathcal{Q}_l(Z_1,Z_2,Z_3)\equiv\int_{-1}^1[(Z_1-\mu)(Z_2-\mu)(Z_3-\mu)]^{-1}P_l(\mu)d\mu, \tag{39}$$

$$Z_{\gamma 2}=-\frac{\mathfrak{M}_\gamma\beta_\gamma^2}{2m_2qq_a}-\frac{\mathfrak{M}_\gamma q_a}{2m_2q}-\frac{m_2q}{2\mathfrak{M}_\gamma q_a}, \tag{40}$$

$$Z_{2\gamma}=Z_{\gamma 2}\quad\text{with}\quad\gamma\leftrightarrow 2\quad\text{and}\quad q\leftrightarrow q_a, \tag{41}$$

$$\bar{Z}_{2\gamma}=Z_{2\gamma}\quad\text{with}\quad\beta_2\rightarrow\alpha_2, \tag{42}$$

$$\alpha_2=(2\mu_2B_2)^{1/2},\quad N_2=8\pi\alpha_2\beta_2(\alpha_2+\beta_2)^3, \tag{43}$$

$$[C_\gamma]=\begin{bmatrix}1/2\\ 0\\ \sqrt{3}/2\end{bmatrix}. \tag{44}$$

In Eqs. (41) and (42) "$\rightarrow$" means "replaced by" and "$\leftrightarrow$" means "interchanged." In Eq. (43), B_2 is the deuteron binding energy.

For each partial wave the matrix $R_{l\alpha\beta}(q,q')$ satisfies the equation

$$R_{l\alpha\beta}(q,q')=K_{l\alpha\beta}(q,q')+\sum_\gamma\int_0^\infty K_{l\alpha\gamma}(q,q'')\tau^\gamma(q'')\times R_{l\gamma\beta}(q'',q')(2\pi)^{-2}(q'')^2dq'', \tag{45}$$

where

$$K_{l\alpha\beta}(q,q')=\mathcal{Q}_l(Z_{\alpha\beta},Z_{\beta\alpha},Z_{\alpha\beta}(E))\left(\frac{\mathfrak{M}_\alpha\mathfrak{M}_\beta m_0}{4m_\alpha m_\beta}\right)\frac{W_{\alpha\beta}}{(qq')^3}, \tag{46}$$

with

$$Z_{\alpha\beta}=Z_{\alpha 2}\quad\text{with}\quad q_2\rightarrow q'\quad\text{and}\quad 2\rightarrow\beta, \tag{47}$$

$$Z_{\beta\alpha}=Z_{\alpha\beta}\quad\text{with}\quad q\leftrightarrow q'\quad\text{and}\quad\alpha\leftrightarrow\beta, \tag{48}$$

$$Z_{\alpha\beta}(E)=\frac{E^+m_0}{qq'}-\frac{\mathfrak{M}_\beta q}{2m_\alpha q'}-\frac{\mathfrak{M}_\alpha q'}{2m_\beta q}, \tag{49}$$

$$[W_{\alpha\beta}]=\begin{bmatrix}-1/2 & 1/\sqrt{2} & \sqrt{3}/2\\ 1/\sqrt{2} & 0 & \sqrt{\frac{3}{2}}\\ \sqrt{3}/2 & \sqrt{\frac{3}{2}} & 1/2\end{bmatrix}, \tag{50}$$

$$E^+=E+i\eta,\quad\eta\rightarrow 0^+;\quad m_0=\mathfrak{M}-m_\alpha-m_\beta. \tag{51}$$

Equations (34) through (51) represent our final equations for the K^--d elastic scattering matrix elements. We have used S-wave NLS potentials of the Yamaguchi form for the two-body interactions. Our method is not restricted to this case, however. The same type of analysis could be carried out if the interactions are generalized to include sums of separable potentials of any reasonable form in more than one angular momentum channel. For such generalizations, the kernel becomes a matrix of larger order, but the basic result that the problem reduces to a set of one-dimensional integral equations still obtains.

B. Method of Solution

For scattering at energies above the threshold for deuteron breakup Eqs. (34) through (51) are not yet in a form that allows a rapid numerical evaluation. The difficulty lies in Eq. (45). In particular there exists a range of values of q, q' such that $K_{l\alpha\beta}(q,q')$ is a rapidly varying function of these variables.

[18] See Appendix B for details of the manipulations mentioned in this paragraph.

[19] As the low-energy K^--N data is fit with a zero range model, the range of the K^--N potential is at our disposal. See the discussion in Sec. III.A.

[20] For analogous results with a scalar "kaon" and distinguishable scalar "nucleons" see L. H. Schick and J. H. Hetherington, *Proceedings of the 1964 Midwest Conference on Theoretical Physics* (to be published).

To see that this is so, we note that from Eq. (39) $\mathcal{Q}_l(Z_{\alpha\beta},Z_{\beta\alpha},Z_{\alpha\beta}(E))$ has branch points at $Z_{\alpha\beta}=\pm 1$, $Z_{\beta\alpha}=\pm 1$, and $Z_{\alpha\beta}(E)=\pm 1$. From Eqs. (40) and (47) $Z_{\alpha\beta}=\pm 1$ yields

$$-\beta_\alpha{}^2=[q'\pm(m_\beta/\mathfrak{M}_\alpha)q]^2, \tag{52}$$

a relation which cannot be satisfied for q, q' real. In fact $Z_{\alpha\beta}+1$ is negative for q, $q'>0$.[21] Similarly, we see from Eqs. (40), (47), and (48) that the branch points at $Z_{\beta\alpha}=\pm 1$ are never reached for q, $q'>0$. On the other hand from Eq. (49) $Z_{\alpha\beta}(E)=\pm 1$ gives

$$(\mathfrak{M}_\beta/m_\alpha)q^2+(\mathfrak{M}_\alpha/m_\beta)q'^2\pm 2qq'-2E^+m_0=0, \tag{53}$$

or, since $(\mathfrak{M}_\beta/m_\alpha)>1$

$$(q+q')^2-2E^+m_0<0. \tag{54}$$

For scattering at an energy below the threshold for deuteron breakup $E<0$, so that even in the limit $\eta\to 0^+$ Eq. (54) cannot be satisfied. For $E>0$ however, there exist values of q, q' for which $Z_{\alpha\beta}(E)$ comes within a distance proportional to η of the branch points at $Z_{\alpha\beta}(E)=\pm 1$. It is for these values of q, q' that $K_{l\alpha\beta}(q,q')$ is a very rapidly varying function of its arguments. At best a large number of points would be required for the numerical representation of $K_{l\alpha\beta}(q,q')$; a large amount of computer time would be needed to obtain a good solution to the set of integral equations given in Eq. (45).

To circumvent this difficulty we allow all the momentum variables to become complex and solve Eq. (45) for q, q', and q'' on contours that are sufficiently far from any singularities. The amplitudes given in Eqs. (36) and (37) are calculated by integrating over the same contours used in the solving of Eq. (45). We make sure that in distorting each contour of integration from its original position along the positive real axis, we do not cross any singularities of the relevant integrand. In such a case Cauchy's theorem insures that the numerical values of $\eta_l{}^{\mathrm{IA}}$ and $\eta_l{}^{\mathrm{MS}}$ remain unchanged.

First we determine suitable contours along which to solve Eq. (45). The behavior of $K_{l\alpha\beta}(q,q')$ may be traced in detail in the q and q' planes, but it is sufficient to consider the behavior of this kernel in the $Z_{\alpha\beta}$, $Z_{\beta\alpha}$, and $Z_{\alpha\beta}(E)$ complex planes.

From Eq. (49) it follows that for a given $q>0$ the contour $0\leq q'\leq\infty$ in the $Z_{\alpha\beta}(E)$ plane has the form shown by curve A of Fig. 1. This contour passes an infinitesimal distance above the branch points at $Z_{\alpha\beta}(E)=\pm 1$. We wish to move this contour away from these branch points into the upper half-$Z_{\alpha\beta}(E)$ plane. Furthermore we wish to perform this distortion of the contour in a manner that treats the variables q and q' symmetrically. Curve A of Fig. 1 holds equally well for fixed $q'>0$ and $0\leq q\leq\infty$; as we must eventually integrate over both q and q' to obtain the scattering amplitude, we want to preserve this symmetry.

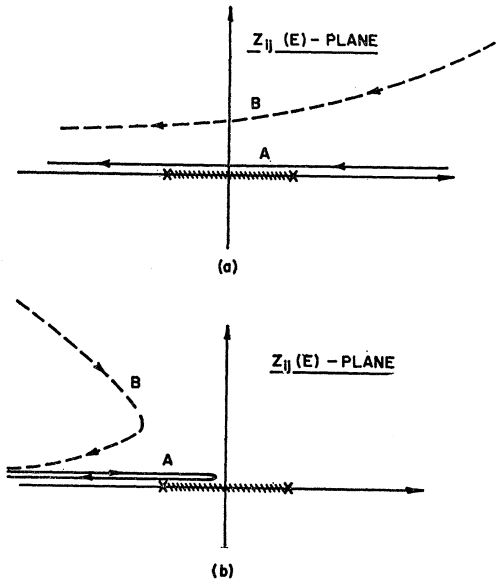

FIG. 1. Loci of $Z_{ij}(E)$ in the complex plane (*a*) for the case $2Em_0m_j>\mathfrak{M}_iq^2$ and (b) for the case $2Em_0m_j<\mathfrak{M}_iq^2$. The curves labeled A are for integration along the real axis, curves labeled B are for integration along the contour described in the text.

We let q and q' become complex by the transformations

$$q\to xe^{-i\phi},\quad q'\to x'e^{-i\phi}, \tag{55}$$

where ϕ is a fixed angle and x, $x'>0$; i.e., in the q plane we rotate the contour $0\leq q\leq\infty$ (about an axis through the origin) an angular distance ϕ into the fourth quadrant and we do likewise to the contour $0\leq q'\leq\infty$ in the q' plane. The angle ϕ is merely a parameter to be chosen such that the new contours lie as far as possible from the singularities of the integrands of Eqs. (36), (37), and (45).

From Eq. (55), Eq. (49) becomes

$$Z_{\alpha\beta}(E)=\frac{m_0Ee^{2i\phi}}{xx'}-\frac{\mathfrak{M}_\beta x}{2m_\alpha x'}-\frac{\mathfrak{M}_\alpha x'}{2m_\beta x}, \tag{56}$$

where, having made use of η to tell us in which direction to move our contour, we have taken the limit $\eta\to 0$. In order to have $\mathrm{Im}Z_{\alpha\beta}(E)>0$ we see from Eq. (56) and the fact that $E>0$ that we must take

$$0<\phi<\pi/2. \tag{57}$$

For fixed x, the new contour $0\leq x'\leq\infty$ is of the form given by curve B of Fig. 1.

To see that we have not crossed any of the other singularities of the integrand of Eq. (45) we combine Eqs. (40), (47), (48), and (55) to obtain

$$Z_{\alpha\beta}=-\frac{\mathfrak{M}_\alpha\beta_\alpha{}^2e^{2i\phi}}{2m_\beta xx'}-\frac{m_\beta x}{2\mathfrak{M}_\alpha x'}-\frac{\mathfrak{M}_\alpha x'}{2m_\beta x}. \tag{58}$$

[21] $Z_{\alpha\beta}\to -1$ as both q and $q'\to\infty$ with $(q'/q)=(m_\beta/\mathfrak{M}_\alpha)$. Other factors in $K_{l\alpha\beta}(q,q')$ cause this limit to give a vanishing contribution to the kernel.

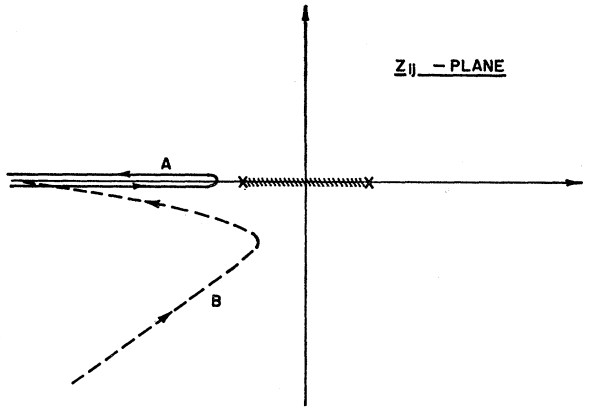

FIG. 2. Loci of Z_{ij}. Curve A is for integration along the real axis, curve B is for integration along the distorted contour.

The branch points of $K_{l\alpha\beta}(q,q')$ and the contour $0\leq q'\leq\infty$ for fixed q (curve A) in the $Z_{\alpha\beta}$ plane are shown in Fig. 2. For $\phi>0$ the contour is distorted into a form such as curve B of Fig. 2. It is clear from Eq. (58) that the branch points are not crossed during such a distortion. By the same argument the branch points of $\bar{K}_{l\alpha\beta}$ at $Z_{\beta\alpha}=\pm1$ have not been crossed either. Finally, it follows from Eqs. (27), (28), and (33) that the "weight function" $\tau^\gamma(q)$ in the integrand of Eq. (45) has no singularities in the fourth quadrant of the complex q plane.

We next consider the integrands of Eqs. (36) and (37). We note that since Eq. (48) is of the Fredholm type it is sufficient to consider Eq. (37) with $R_{l\alpha\beta}(q,q')$ replaced by $K_{l\alpha\beta}(q,q')$. The only functions on the right of Eqs. (36) and (37) that we have not discussed are $\Phi_{l\gamma2}(q,q_a)$ and $\Phi_{l\beta2}(q',q_a)$.

From Eqs. (38) and (39) $\Phi_{l\gamma2}$ has branch points at $Z_{\gamma2}=\pm1$, $Z_{2\gamma}=\pm1$, and $\bar{Z}_{2\gamma}=\pm1$. With $Z_{\gamma2}=\pm1$, Eq. (45) gives

$$q=(\mathfrak{M}_\gamma/m_2)[\pm q_a\pm i\beta_\gamma], \tag{59}$$

where from Eqs. (38) and (44) we need only consider $\gamma=1$ or 3. Since q_a is the magnitude of the kaon momentum in the final (or initial) state, $\Phi_{l\gamma2}(q,q_a)$ has a branch point in the fourth quadrant of the q plane. With ϕ_1 as the angle between the positive real axis and the line from the origin to this branch point, we have from Eq. (59),

$$\phi_1=-\tan^{-1}(\beta_\gamma/q_a),\quad \gamma=1,3. \tag{60}$$

Similarly from the branch point at $Z_{2\gamma}=\pm1$, we obtain a branch point in the fourth quadrant of the q plane that lies at an angle

$$\phi_2=-\tan^{-1}(\mathfrak{M}_2\beta_2/m_\gamma q_a),\quad \gamma=1,3, \tag{61}$$

with respect to the positive real axis. The branch point at $\bar{Z}_{2\gamma}=\pm1$ gives a branch point that lies at an angle

$$\phi_3=-\tan^{-1}(\mathfrak{M}_2\alpha_2/m_\gamma q_a),\quad \gamma=1,3, \tag{62}$$

with respect to the positive real axis. We let $\phi_{\max}$ be the smallest of $|\phi_i|$, $i=1$, 2, 3. For $\phi<\phi_{\max}$ our rotated contour in the q plane will not have crossed any of these branch points. An identical analysis of $\Phi_{l\beta2}(q',q_a)$ holds in the q' plane.

Finally we note that the integrands of Eqs. (36) and (37) vanish fast enough at large q (or q') that when we join each rotated contour to the corresponding positive real axis by an arc of infinite radius, the value of each integral along such an arc is zero. Thus, the numerical values of $\eta_l^{\rm IA}$ and $\eta_l^{\rm MS}$ are the same when the integrals are evaluated along the rotated contours as when they are evaluated along the original contours.

III. RESULTS

A. Preliminary Computations

Before any computations could be performed, the parameters of the two-body potentials had to be fixed. The parameters chosen for the n-p spin triplet potential were those given in Ref. 14:

$$\alpha_2=45.706\ \text{MeV}/c,\quad \beta_2=6.255\alpha_2. \tag{63}$$

The selection of the kaon-nucleon scattering parameters was not so straightforward.

The low energy K-N data is fit with a zero-range model.[22] The Humphrey and Ross (H. R.) solutions for the isospin singlet (A_0) and triplet (A_1) scattering lengths are[14]

$$\begin{aligned}&\text{I.}\quad A_0=(-0.22+i2.74)\ \text{F},\quad A_1=(0.02+i0.38)\ \text{F},\\&\text{II.}\quad A_0=(-0.59+i0.96)\ \text{F},\quad A_1=(1.20+i0.56)\ \text{F}.\end{aligned} \tag{64}$$

The model we used had a complex strength parameter and a real range parameter for each isospin channel; i.e., we had two arbitrary range parameters $\beta^{-1}(0)$ and $\beta^{-1}(1)$. However, we reduced the number of free parameters to one real parameter β^{-1} by taking the range to be the same for both isospin channels. We then found that for relative momenta in the region ($\lesssim150$ MeV/c) where multiple scatterings should be most important, with the H. R. II solutions the K-N scattering in both channels was dominated by the contribution from the scattering length when we chose $\beta^{-1}\lesssim0.4$ F. For the H. R. I solutions and the same range of momenta, the scattering lengths dominated for $\beta^{-1}\lesssim0.1$ F. As the value for the range parameter seemed the more physically reasonable, most of the computations were performed with the H. R. II solutions and $\beta^{-1}=0.4$ F.

Several further preliminaries were performed before the main computations were undertaken. To reduce the integrals in Eqs. (36), (37), and (45) to a more con-

[22] J. D. Jackson, D. G. Ravenhall, and H. W. Wyld, Nuovo Cimento 9, 834 (1958); R. H. Dalitz and S. F. Tuan, Ann. Phys. 8, 100 (1959).

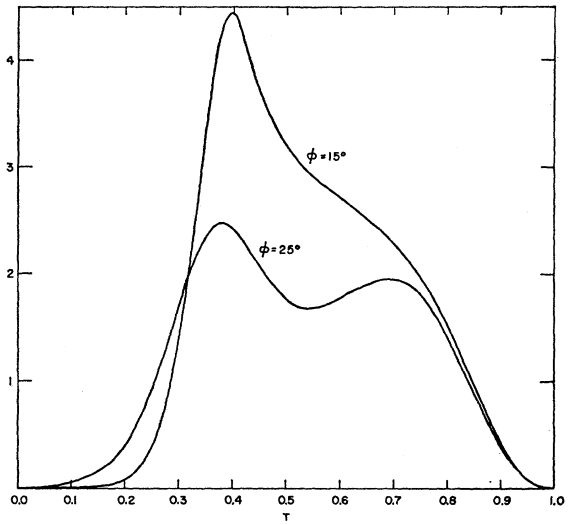

FIG. 3. The real part of $\kappa_{0,2,3}(T,T)$ for $p_0=194$ MeV/c, $\beta^{-1}=0.4$ F, H.R. solution II for two different values of the angle ϕ. The strong peaking as the angle ϕ becomes smaller is evident. The ordinate is in arbitrary units.

venient form we made the substitutions

$$q=xe^{-i\phi}=e^{-i\phi}V_cT(1-T)^{-1},$$
$$q'=x'e^{-i\phi}=e^{-i\phi}V_cT'(1-T')^{-1}. \tag{65}$$

When expressed in terms of T, T', etc., the integrals were now over the finite range 0 to 1. The arbitrary constant V_c was chosen so that the structure of each integrand was near the middle of this range. The value $V_c\approx 1.5q_a$ gave satisfactory results in this respect. Also for numerical convenience we worked with the functions

$$\kappa_{l\alpha\beta}(T,T')\propto(xx')^2(TT')^{-1}K_{l\alpha\beta}(xe^{-i\phi},x'e^{-i\phi}), \tag{66}$$

$$\Psi_{l\alpha 2}(T,q_a)\propto x^2T^{-1}\Phi_{l\alpha 2}(xe^{-i\phi},q_a), \tag{67}$$

rather than $K_{l\alpha\beta}$ and $\Phi_{l\alpha 2}$. This choice eliminated the appearance of ∞ times zero in the limit $T\to 1$ and simplified the "weight function" appearing in each integrand.

Before computing the cross sections themselves we investigated numerically[23] the behavior of various parts of the integrands of Eqs. (36), (37), and (45). We present below some of the results of these computations.

To illustrate the effect of the variation of the angle ϕ on the kernel of our integral equation we show in Fig. 3 the real part of $\kappa_{023}(T,T)$ at $p_0=194$ MeV/c[24] with $\beta^{-1}=0.4$ F and the H. R. II solutions for A_0 and A_1. Note that as ϕ is decreased the peaking at $T=0.4$ becomes more pronounced. This is the peak due to the approach of $Z_{23}(E)$ to the branch cut $-1\leq Z_{23}(E)\leq+1$. If ϕ were taken to be vanishingly small, this peak would become discontinuous at two places corresponding to the two branch points at the ends of the cut.

Figure 4 is a contour plot of the real part of $\kappa_{023}(T,T')$ for the same values of the parameters as were used on Fig. 3, but with $\phi=15°$. (The 15° curve in Fig. 3 is just the profile along the diagonal of this three-dimensional plot.) The dotted curves are the solutions of $Z_{23}(E)=\pm 1$ for $\phi=0$. The effect of these nearby singularities is evident. For higher values of l the kernel $\kappa_{l23}(T,T')$ oscillates in the region between these two curves due to the presence of $P_l(\mu)$ in the integral representation of $\mathcal{Q}_l$ given in Eq. (39).

As pointed out in Sec. II. B, $\Phi_{l\alpha 2}(q,q_a)$ has a branch cut in the q plane that places an upper limit on the angle ϕ.[25] The function $\Psi_{012}(T,q_a)$ for the same set of parameters as were used above is presented for various ϕ in Fig. 5. In this case $\phi_{\max}=30.6°$. Again we see that sharp peaking occurs as we approach the branch point.

Actual computational experience showed that for $p_0=194$ MeV/c ($\phi_{\max}=30.6°$) a value of ϕ in the range 10–15° was the best compromise. With this ϕ the kernel $\kappa_{l\alpha\beta}(T,T')$ and $\Psi_{l\alpha 2}(T,q_a)$ for those l which contributed significantly to the scattering amplitude were found to be accurately represented by a mesh of 39 points in each variable T and T'. This mesh size was also found to be satisfactory at the other momenta $-p_0=105$ MeV/c and $p_0=300$ MeV/c—at which computations were performed.

With this mesh a computation of the elastic angular

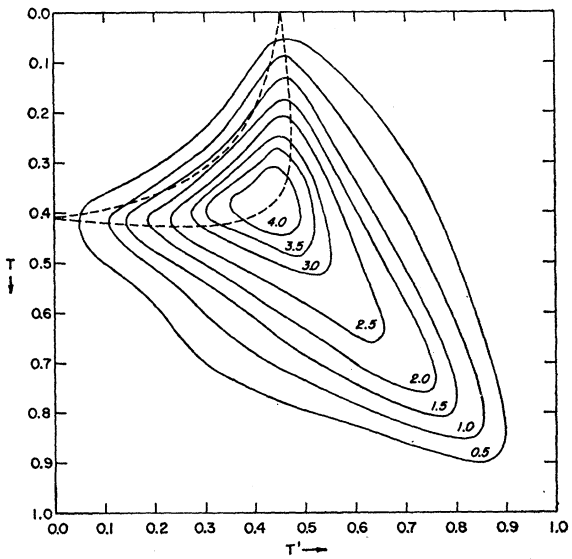

FIG. 4. The real part of $\kappa_{0,2,3}(T,T')$ for $p_0=194$ MeV/c, $\beta^{-1}=0.4$ F, H.R. solution II, $\phi=15°$. The altitude contours are in the same units as the ordinate in Fig. 3. The dotted curves are solutions of $Z_{ij}(E)=\pm 1$ for $\phi=0°$ and represent the location of the discontinuities in the function κ when $\phi=0°$. Note that the T scale increases toward the bottom and the T' scale increases toward the right in conformity with the numbering of rows and columns in a matrix.

[23] All numerical work was performed on a CDC 1604.

[24] Nonrelativistically the incident-kaon lab momenta p_0 of 300, 194 and 105 MeV/c correspond to the three-particle center-of-mass energies of 69.93, 27.95, and 6.614 MeV, respectively.

[25] For the ranges we have used, $\phi_{\max}$ is determined by Eq. (65).

distribution, elastic cross section, and total cross section for a given energy and a given set of K-N parameters was found to take about 20 min on a CDC 1604. A different numerical scheme than the one used could be devised which would allow for the computation of the integrals in Eq. (37) on a finer mesh than the mesh used to solve the integral equation. This would allow ϕ to be increased to a value nearer ϕ_{max} making the kernel of the integral equation even more slowly varying. Since the solving of the integral equation is inherently a more time consuming operation than the evaluation of the final integrals, the computation time would be shortened. We felt that such efforts would be worth while for more complicated potentials—such as sums of NLS potentials—than those used here. For the present problem, however, no great numerical sophistication was necessary.

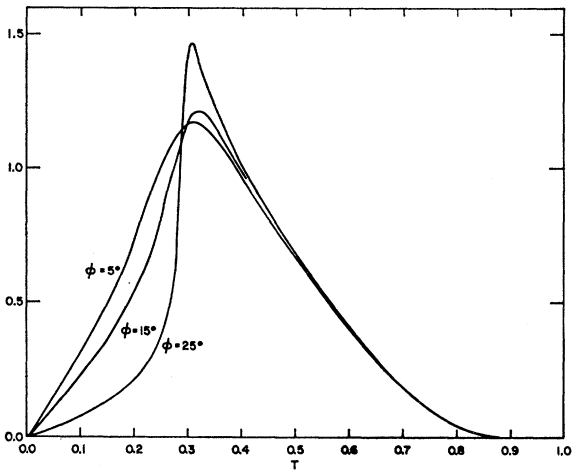

FIG. 5. The real part of $\Psi_{0,1,2}(T)$ for $p_0=194$ MeV/c, $\beta^{-1}=0.4$ F, H.R. solution II. Here the presence of the branch point at $\phi=30.6°$ is manifest by the increasingly rapid variation of the function as ϕ increases.

B. Cross Sections

The elastic angular distribution, elastic, total, and reaction cross sections, respectively, were calculated according to the following formulas:

$$(d\sigma_{el}/d\Omega)=(\mu_{Kd}/2\pi)^2|\sum(2l+1)\eta_l P_l(\hat{q}_a\cdot\hat{q}_b)|^2, \quad (68)$$

$$\sigma_{el}=(\mu_{Kd}{}^2/\pi)\sum(2l+1)|\eta_l|^2, \quad (69)$$

$$\sigma_{tot}=-(2\mu_{Kd}/q_a)\sum(2l+1)\,\mathrm{Im}(\eta_l), \quad (70)$$

$$\sigma_{react}=\sigma_{tot}-\sigma_{el}, \quad (71)$$

where μ_{Kd} is the kaon-deuteron reduced mass. These quantities were calculated in the impulse approximation (IA), the double scattering approximation (DS), and with the exact multiple scattering equations (MS). For the impulse approximation η_l in Eqs. (68) through (70) was taken to be $\eta_l{}^{IA}$ given by Eq. (36). For the multiple scattering case, we used $\eta_l=\eta_l{}^{IA}+\eta_l{}^{MS}$ with Eqs. (36)

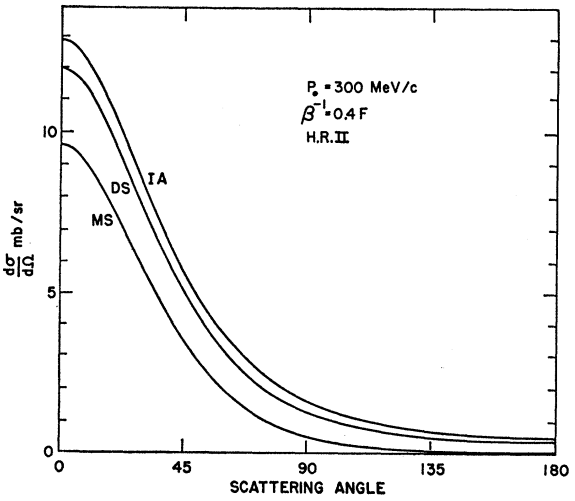

FIG. 6. K^--d elastic differential cross section for kaon lab momentum $p_0=300$ MeV/c, $\beta^{-1}=0.4$ F, using the H.R. solution II. The curve labeled IA is the impulse approximation, the curve DS contains double scattering corrections, MS labels the exact multiple-scattering curve.

and (37). The double scattering approximation $\eta_l=\eta_l{}^{IA}+\eta_l{}^{DS}$ was obtained through the replacement of $R_{l\alpha\beta}(q,q')$ in Eq. (37) by $K_{l\alpha\beta}(q,q')$. We found that for all cases we could cutoff the partial-wave sums after $l=7$ for the IA contribution, after $l=3$ for the DS contribution, and after $l=1$ for the MS contribution without introducing an error $\gtrsim 1\%$ in any of the computed quantities. These then were the maximum values of l used in Eqs. (68) through (70).

In Table I we list the cross sections that were calculated for various sets of K-N parameters at the three kaon lab momenta used. Column 5 of this table indicates the appropriate figure number for the corresponding angular distribution.

From the elastic angular distributions Figs. 6. 7, 8,

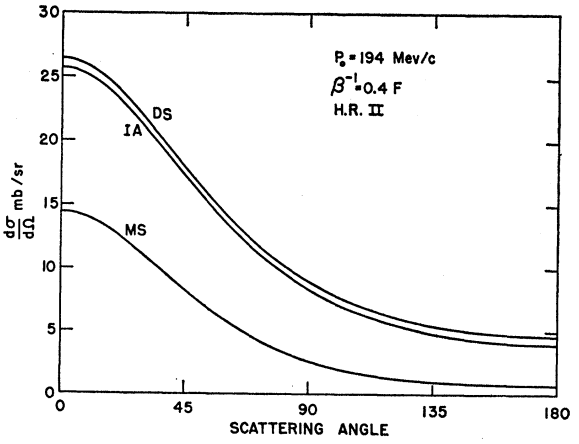

FIG. 7. K^--d elastic differential cross section for kaon lab momentum $p_0=194$ MeV/c, $\beta^{-1}=0.4$ F, using the H.R. solution II. The curve labeled IA is the impulse approximation, the curve DS contains double scattering corrections, MS labels the exact multiple scattering curve.

TABLE I. Elastic and total cross sections for K^--d scattering at various kaon lab momenta and for different potential parameters. Values are given for the impulse approximation (IA), double scattering approximation (DS) and the exact multiple-scattering case.

	β^{-1} (F)	H.R.	p_0 (MeV/c)	Fig. for $d\sigma/d\Omega$	σ_{el} (mb) IA	DS	MS	σ_{tot} (mb) IA	DS	MS
1	0.4	II	300	6	35.1	30.3	18.6	96.2	101	85.1
2	0.4	II	194	7,10	128	136	50.4	209	240	171
3	0.4	II	105	8	346	493	138	434	604	379
4	0.2	II	194	10	164	189	49.6	240	282	182
5	0.1	II	300		64.7	59.4	24.0	141	147	114
6	0.1	II	194	10	177	206	44.4	252	296	180
7	0.1	II	105		383	592	88.2	454	655	317
8	0.1	I	300	11	28.8	23.7	16.4	103	99.3	90.0
9	0.1	I	194	12	84.9	75.5	40.2	204	199	163
10	0.1	I	105	13	245	235	100	488	489	347

11, 12, and 13, it is clear that the major contribution of the double and multiple scatterings is in the $l=0$ channel. The effects of diffraction scattering from the deuteron wave function are evident as E increases—compare Figs. 6, 7, and 8—but the main contribution to this effect comes from the single-scattering term. From Figs. 6, 7, and 8 there seems to be no obvious correlation as to the size of the IA, DS, and MS results. However, in Fig. 9 we have plotted the contributions of the impulse approximation, double scatterings, and higher multiple scatterings to η_0 for each of the three energies. From this diagram an orderly progression from one energy to the next is apparent.

Table II shows η_l^{IA}, η_l^{DS}, and η_l^{MS} for the sets of parameters used in lines 1, 2, 3 of Table I. Again we see that the MS (and DS) contributions are strongest in the $l=0$ channel. Furthermore, for larger l we see that $\eta^{MS} \rightarrow \eta^{DS}$ which indicates that for these l the solution of Eq. (45) can be well approximated by the inhomogeneous term. This is not unexpected. For $l>0$ the kernel becomes smaller in the sense that η_l^{DS} becomes smaller. For a "small" kernel the Liouville-Neuman series should converge rapidly.

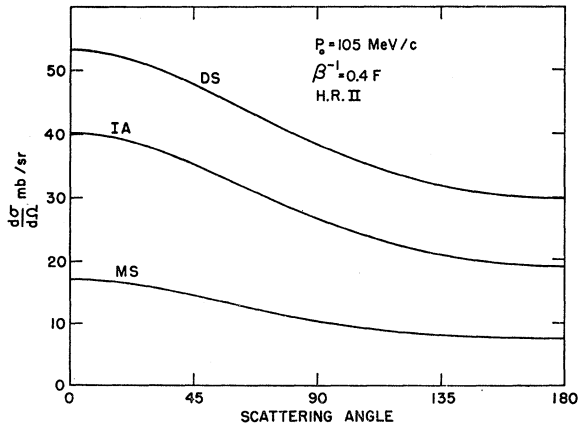

FIG. 8. K^--d elastic differential cross section for kaon lab momentum $p_0=105$ MeV/c, $\beta^{-1}=0.4$ F, using the H.R. solution II. The curve labeled IA is the impulse approximation, the curve DS contains double scattering corrections, MS labels the exact multiple-scattering curve.

TABLE II. Values of η_l^{IA}, η_l^{DS}, η_l^{MS} for $\beta^{-1}=0.4$ F, H.R. solution II at the three kaon lab momenta 300, 194, and 105 MeV/c. The entries in the table are in units of 10^{-5} MeV^{-2}.

p_0 (MeV/c)	l	η_l^{IA}	η_l^{DS}	η_l^{MS}
300	0	$-2.302-3.131i$	$1.411-0.213i$	$1.186+0.976i$
	1	$-0.587-0.815i$	$-0.074-0.057i$	$-0.066-0.044i$
	2	$-0.157-0.222i$	$-0.0027+0.0048i$	$-0.0027+0.0049i$
	3	$-0.047-0.067i$	$-0.0003+0.0004i$	
	4	$-0.016-0.022i$		
	5	$-0.005-0.008i$		
	6	$-0.002-0.003i$		
194	0	$-4.757-6.359i$	$2.705-1.536i$	$3.497+1.901i$
	1	$-0.709-0.984i$	$-0.115-0.024i$	$-0.101-0.016i$
	2	$-0.120-0.173i$	$-0.0006+0.0053i$	$0.0006+0.0053i$
	3	$-0.024-0.035i$	$-0.0004-0.0000i$	
	4	$-0.005-0.008i$		
	5	$-0.001-0.002i$		
105	0	$-9.257-9.738i$	$2.415-4.809i$	$9.018+1.340i$
	1	$-0.568-0.611i$	$-0.067+0.054i$	$-0.055+0.051i$
	2	$-0.043-0.048i$	$-0.002+0.000i$	
	3	$-0.004-0.005i$		
	4	$-0.000-0.000i$		

The "range-dependence" of the angular distribution is shown in Fig. 10. The three curves were calculated at $p_0=194$ MeV/c using the exact theory, the H. R. II

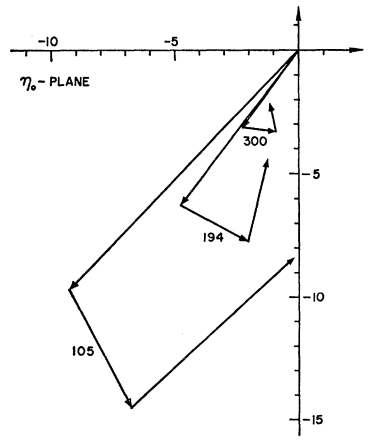

FIG. 9. The contributions to the complex number η_0 from the impulse approximation, double scattering and *higher* multiple scattering for the $\beta^{-1}=0.4$ F, H.R. solution II case at each of the three momenta 300, 194, and 105 MeV/c. For each momentum the arrow beginning at the origin is the impulse approximation η_0^{IA}, the second arrow is the double-scattering term η_0^{DS} and the third arrow is the higher multiple-scattering term $\eta_0^{MS}-\eta_0^{DS}$.

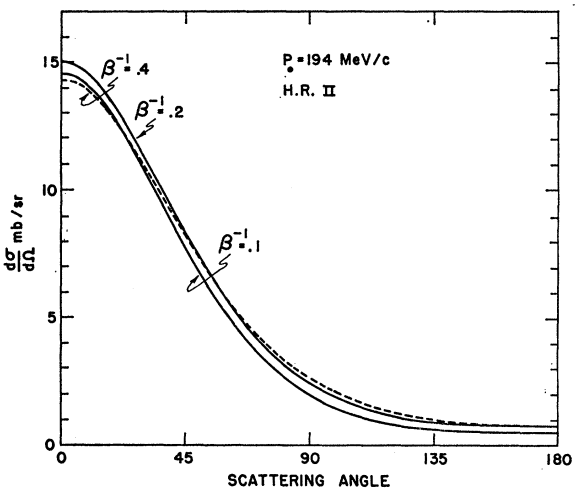

FIG. 10. K^--d elastic differential cross sections at kaon lab momentum 194 MeV/c for the H.R. solution II and for three values of the range. All multiple scattering is included.

solutions, and K-N ranges $\beta^{-1}=0.4$, 0.2, and 0.1 F, respectively. These angular distributions and the corresponding cross sections given in rows 2, 4, and 6 of Table I are clearly not sensitive to the value of β^{-1} used. Unfortunately the more and more rapidly varying nature of $K_{l\alpha\beta}(q,q')$ for large q and q' as β^{-1} becomes smaller and smaller prevented our continuing the investigation to values of $\beta^{-1}<0.1$ F without the use of a finer mesh and a more sophisticated program. Although such modifications are easily carried out, we have not done so at this time. We do not claim, therefore, that we have reached the "zero-range" limit. A direct comparison of our results with calculations using a "zero-range" interaction may be somewhat questionable.

Figures 11, 12, and 13 show the elastic angular distribution at momenta $p_0=300$, 194, and 105 MeV/c, respectively, for the case of $\beta^{-1}=0.1$ F with the H. R. I solutions for the scattering lengths.

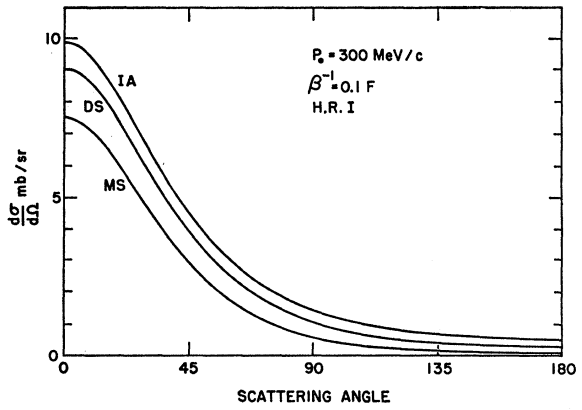

FIG. 11. K^--d elastic differential cross section at kaon lab momentum $p_0=300$ MeV/c, $\beta^{-1}=0.1$ F, for the H.R. solution I. The labels IA, DS, and MS refer to impulse approximation, double scattering, and multiple scattering, respectively.

From a perusal of Table I in its entirety we may make some further statements. First, for the elastic cross section the MS "corrections" to the impulse approximation are very large at the smallest value of p_0 investigated [$\sigma^{MS}\approx(0.23-0.40)\sigma^{IA}$ for the H. R. II solutions] and are still large [$\sigma^{MS}\approx(0.37-0.53)\sigma^{IA}$] at $p_0=300$ MeV/c. At this latter value of p_0, however, the MS corrections to the reaction cross section are of the opposite sign to the corrections to σ_{el} so that the corrections to the total cross section are fairly small ($\approx 10\%$). The double scattering corrections to the impulse approximation results are either fairly small ($\approx 10\%$) or are in the wrong direction, i.e., the DS results are no better and at times are worse approximations to the MS results than is the impulse approximation. The higher (above double) multiple scatterings make a large contribution to the S-wave scattering amplitude in comparison with double scattering. This is evident from

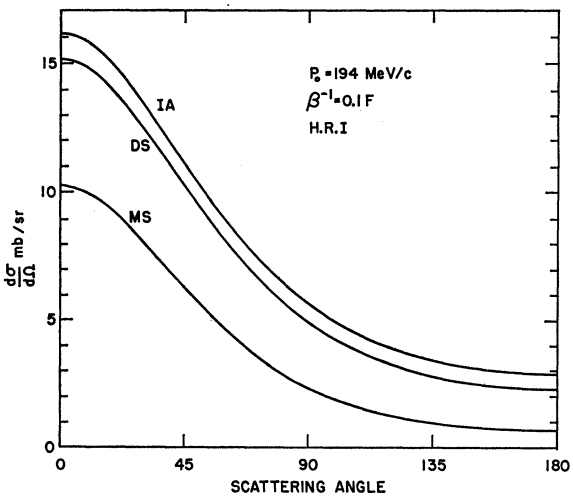

FIG. 12. K^--d elastic differential cross section at kaon lab momentum $p_0=194$ MeV/c, $\beta^{-1}=0.1$ F, for the H.R. solution I. The labels IA, DS, and MS refer to impulse approximation, double scattering, and multiple scattering, respectively.

Fig. 9 as well as from the effects of multiple scattering on the various cross sections presented. Calculations have shown that the largest contributions to multiple scattering come from terms in which a scattering between the two nucleons takes place. It is therefore quite clear that our impulse approximation is quite different, numerically, from the impulse approximation given by Watson[26] where all such scatters are included in the "single scattering" term. Our double scattering term cannot contain any such scatters and is probably much smaller than the third-order multiple scattering term which does. Thus our double scattering term is not comparable to double scattering as calculated in Ref. 8 since these authors include such interactions in double scattering by using the interacting two-nucleon propagator.

[26] K. M. Watson, Phys. Rev. **105**, 1388 (1957).

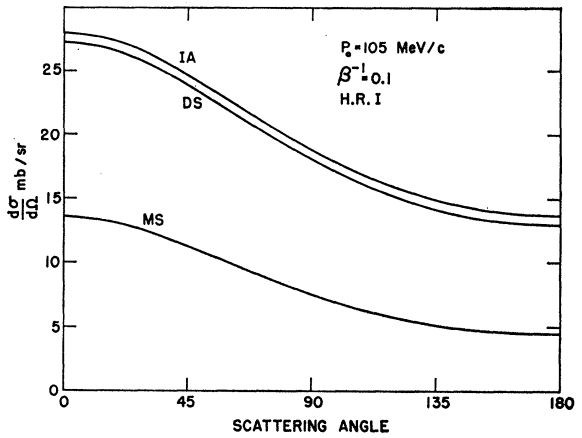

FIG. 13. K^--d elastic differential cross section at kaon lab momentum $p_0=105$ MeV/c, $\beta^{-1}=0.1$ F, for the H.R. solution I. The labels IA, DS, and MS refer to impulse approximation, double scattering, and multiple scattering, respectively.

The results for σ_{el} and σ_{tot} are range-dependent enough to mask the differences between the results for the H. R. I solutions and those for the H. R. II solutions. In any case these differences are smaller than those of previous calculations.[3,8] The ambiguity in the K-N scattering lengths may not be as easily resolved by K^--d scattering experiments as had been previously supposed.

IV. SUMMARY

We have presented a multiple-scattering formalism for low-energy K-d elastic scattering. We assumed that all two-body interactions were separable S-wave potentials of the Yamaguchi form and that the K-N range was isospin independent. Coulomb forces and the K^--$\bar{K}^0$ and n-p mass differences were neglected. A method for performing a rapid numerical evaluation of the scattering amplitude at energies above the threshold for deuteron breakup was derived.

Results were presented for calculations of the elastic angular distribution, elastic cross section and total cross section for incident lab momenta of 105, 194, and 300 MeV/c. These calculations were performed with both the Humphrey and Ross I and II scattering lengths and with K-N "ranges" from 0.1 to 0.4 F. From these results we made the following conclusions:

(i) The major contributions of the double scattering and multiple scattering terms are to S-wave scattering.

(ii) For higher partial waves, the impulse approximation is dominant while the double scattering terms account for the bulk of the multiple-scattering contribution.

(iii) Only for σ_{tot} at 300 MeV/c could the multiple-scattering and double-scattering effects be considered corrections (i.e., $\lesssim 10\%$). For σ_{el} at 300 MeV/c and for both σ_{el} and σ_{tot} at the lower kaon lab momenta the impulse approximation and double scattering results were at best within a factor 2 or 3 of the correct multiple scattering answer.

ACKNOWLEDGMENT

We wish to thank the staff of the University of Minnesota Numerical Analysis Center for their kind cooperation.

APPENDIX A

Equation (24) gives the matrix elements of the free Green's function between a state of the kth "natural" coordinate system on the right and a state of the ith "natural" coordinate system on the left. In order to obtain a consistent set of such matrix elements we must specify each natural coordinate system, being especially careful to define its phase.[27] To form the isospin part of the three basic sets we couple two of the particles to form the total isospin of a pair, then couple this to the third particle to form the total isospin of the system. The ith natural state is then denoted by its total isospin ρ, the z component of total isospin and the total isospin of the ith pair I. To define the phase of the coupled state, we must specify the order of the coupling of the individual isospin into each coupled state. The uncoupled basis set is defined as the product of each of the individual isospin states and is labeled by X, Y, Z, the z components of each of the individual isospins S_1, S_2, S_3, respectively. In order to make our choise of phases explicit, the following equations, which define the three natural, isospin states, are presented:

$$|\rho,\zeta,I_1\rangle=\sum_{X,Y,Z}{}' C(S_2,S_3,I_1;\,Y,Z) \times C(S_1,I_1,\rho;\,X,\,Y+Z)|X,Y,Z\rangle, \quad \text{(A1)}$$

$$|\rho,\zeta,I_2\rangle=\sum_{X,Y,Z}{}' C(S_1,S_3,I_2;\,X,Z) \times C(S_2,I_2,\rho;\,Y,\,X+Z)|X,Y,Z\rangle, \quad \text{(A2)}$$

$$|\rho,\zeta,I_3\rangle=\sum_{X,Y,Z}{}' C(S_1,S_2,I_3;\,X,Y) \times C(I_3,S_3,\rho;\,X+Y,\,Z)|X,Y,Z\rangle. \quad \text{(A3)}$$

Here I_1, I_2, I_3 are the isospin of the pairs 23, 13, 12, respectively, and the primes on the summations indicate that the summation is restricted by the condition $X+Y+Z=\zeta$. The C's are the Clebsch-Gordan coefficients as defined by Rose.[28]

We wish to take matrix elements of the isospin part of the free Green's function. The 3-components of the isospin enter the expression, Eq. (22), for the matrix elements of the Green's function between uncoupled states only in the product $\delta_{X,X'}\delta_{Y,Y'}\delta_{Z,Z'}$. For this reason, the product $\delta_{\rho,\rho'}\delta_{\zeta,\zeta'}U^{ik}(I,K)$ appearing in Eq. (24) is given by

$$\langle\rho,\zeta,I|\sum_{X,Y,Z}|X,Y,Z\rangle\langle X,Y,Z|\rho',\zeta',K\rangle. \quad \text{(A4)}$$

[27] A. R. Edmonds, *Angular Momentum in Quantum Mechanics* (Princeton University Press, Princeton, New Jersey, 1957).

[28] M. E. Rose, *Elementary Theory of Angular Momentum* (John Wiley & Sons. Inc., New York, 1957).

Here the state on the left is in the ith natural set while the state on the right is in the kth natural set. Combining Eq. (A4) with Eqs. (A3) and (A1) we obtain

$$U^{31}(K,I)=\sum_{X,Y,Z}{}' C(S_1,S_2,K;X,Y)C(K,S_3,\rho;X+Y,Z) \times C(S_2,S_3,I;Y,Z)C(S_1,I,\rho;X,Y+Z) =[(2K+1)(2I+1)]^{1/2}W(S_1,S_2,\rho,S_3;K,I),$$

where W is the Racah coefficient as defined in Chap. 6 of Rose. Similar considerations yield

$$U^{12}(I,J)=(-1)^{2S_1+I-\rho+S_3-J} \times[(2I+1)(2J+1)]^{1/2}W(S_2,S_3,\rho,S_1;I,J)$$

and

$$U^{32}(K,J)=(-1)^{S_1+S_2-K} \times[(2K+1)(2J+1)]^{1/2}W(S_2,S_1,\rho,S_3;K,J).$$

Now in K^--d scattering $S_1=S_2=S_3=1/2$ so that the expressions

$$[U^{31}(K,I)]=[U^{13}(I,K)]=\begin{bmatrix}-1/2 & \sqrt{3}/2\\ \sqrt{3}/2 & 1/2\end{bmatrix}, \quad \text{(A5)}$$

$$[U^{12}(I,J)]=[U^{21}(J,I)]=\begin{bmatrix}1/2 & \sqrt{3}/2\\ \sqrt{3}/2 & -1/2\end{bmatrix}, \quad \text{(A6)}$$

$$[U^{23}(J,K)]=[U^{32}(K,J)]^{\dagger}=\begin{bmatrix}1/2 & \sqrt{3}/2\\ -\sqrt{3}/2 & 1/2\end{bmatrix}. \quad \text{(A7)}$$

give the explicit numerical values of $U^{ik}(I,K)$ for the case of K^--d scattering.

APPENDIX B

Substituting Eq. (28) into Eq. (26) and factoring out $v_i(k_i,I)$ on the left and $\tau_j(q_j',J)v_j(k_j',J)$ on the right, we obtain

$$T^{ij}(\mathbf{q}_i,I;\mathbf{q}_j',J')=(2\pi)^3\delta(\mathbf{q}_i-\mathbf{q}_j')\delta_{i,j}\delta_{I,J'} +\sum_{k=1}^{3}\sum_{K''=0}^{1}\int\frac{d\mathbf{q}_k''}{(2\pi)^3}K^{ik}(\mathbf{q}_i,I;\mathbf{q}_k'',K'') \times\tau_k(q_k'',K'')T^{kj}(\mathbf{q}_k'',K'';q_j',J'), \quad \text{(B1)}$$

where

$$\langle\mathbf{q}_i,\mathbf{k}_i;I|T^{ij}|\mathbf{q}_j',\mathbf{k}_j';J'\rangle =v_i(k_i,I)T^{ij}(\mathbf{q}_i,I;\mathbf{q}_j',J')\tau_j(q_j,J')v_j(k_j,J'), \quad \text{(B2)}$$

with

$$K^{ij}(\mathbf{q}_i,I;\mathbf{q}_j',J')=D^{-1}(\mathbf{q}_i,\mathbf{q}_i+\mathbf{q}_j',\mathbf{q}_j')U^{ij}(I,J')(1-\delta_{i,j}) \times v_i(\mp(m_j/\mathfrak{M}_i)\mathbf{q}_i\mp\mathbf{q}_j',I) \times v_j(\mp\mathbf{q}_i\mp(m_i/\mathfrak{M}_j)\mathbf{q}_j',J'). \quad \text{(B3)}$$

Since none of the interactions can cause spin flip of the nucleons, the nucleons are always in a relative spin triplet state. Thus the interaction in the isospin triplet state will be absent because we have only included S-wave interactions and the space part of the wave function cannot be an S wave in this case. We may therefore set the potential $v_2(k,1)$ equal to zero.

Since particles 1 and 3 are identical and the isospin triplet nucleon-nucleon potential is zero

$$K^{23}(\mathbf{q}_2,J;\mathbf{q}',K')=K^{21}(\mathbf{q}_2,J;\mathbf{q}',K')$$
$$K^{32}(\mathbf{q},K;\mathbf{q}_2',J')=K^{12}(\mathbf{q},K;\mathbf{q}_2',J')$$

and

$$K^{31}(\mathbf{q},K;\mathbf{q}',K')=K^{13}(\mathbf{q},K;\mathbf{q}',K')$$

The matrix-integral equation (B1) can therefore be written symbolically as:

$$\begin{bmatrix}T^{11} & T^{12} & T^{13}\\ T^{21} & T^{22} & T^{21}\\ T^{13} & T^{12} & T^{11}\end{bmatrix}=\begin{bmatrix}1 & 0 & 0\\ 0 & 1 & 0\\ 0 & 0 & 1\end{bmatrix}+\begin{bmatrix}0 & K^{12} & K^{13}\\ K^{21} & 0 & K^{21}\\ K^{13} & K^{12} & 0\end{bmatrix}\times\begin{bmatrix}\tau_1 & 0 & 0\\ 0 & \tau_2 & 0\\ 0 & 0 & \tau_1\end{bmatrix}\times\begin{bmatrix}T^{11} & T^{12} & T^{13}\\ T^{21} & T^{22} & T^{21}\\ T^{13} & T^{12} & T^{11}\end{bmatrix}. \quad \text{(B4)}$$

According to Eq. (7), the entire scattering matrix T is given by

$$T=2v_1(k,I)[T^{11}(\mathbf{q},I;\mathbf{q}',I')+T^{31}(\mathbf{q},I;\mathbf{q}',I')]\tau_1(q',I')v_1(k',I'). \quad \text{(B5)}$$

Since only the sum $T^{11}+T^{31}$ is needed for the evaluation of T, Eq. (B4) can be reduced to

$$\begin{bmatrix}T^{22} & \sqrt{2}T^{21}\\ \sqrt{2}T^{12} & (T^{11}+T^{13})\end{bmatrix}=\begin{bmatrix}1 & 0\\ 0 & 1\end{bmatrix}+\begin{bmatrix}0 & \sqrt{2}K^{21}\\ \sqrt{2}K^{12} & K^{13}\end{bmatrix}\times\begin{bmatrix}\tau_2 & 0\\ 0 & \tau_1\end{bmatrix}\times\begin{bmatrix}T^{22} & \sqrt{2}T^{21}\\ \sqrt{2}T^{12} & (T^{11}+T^{33})\end{bmatrix}. \quad \text{(B6)}$$

Now each of the elements of the matrices in Eq. (B6) is itself 2×2 matrix in isospin space. Since the isospin-1 potential is zero in the nucleon-nucleon channel, however, T^{22} has only one nonzero element and $T^{12}=\tilde{T}^{21}$ has only one nonzero row. Therefore, when the matrix equation (B6) is expanded to explicitly represent the isospin dependence of its elements, it becomes an equation in only 3×3 matrixes. The kernel in Eq. (B6) when written out explicitly is thus

$$\begin{bmatrix}0 & \sqrt{2}K^{21}(\mathbf{q},0;\mathbf{q}',0) & \sqrt{2}K^{21}(\mathbf{q},0;\mathbf{q}',1)\\ \sqrt{2}K^{12}(\mathbf{q},0;\mathbf{q}',0) & K^{13}(\mathbf{q},0;\mathbf{q}',0) & K^{13}(\mathbf{q},0;\mathbf{q}',1)\\ \sqrt{2}K^{12}(\mathbf{q},1;\mathbf{q}',0) & K^{13}(\mathbf{q},1;\mathbf{q}',0) & K^{13}(\mathbf{q},1;\mathbf{q}',1)\end{bmatrix}. \quad \text{(B7)}$$

The subscripts on the variables q have been dropped here since they are dummy variables. The elements of the matrix (B7) are denoted by $K_{\alpha\beta}(q,q')$ where α, β refer to rows and columns in (B7) but such that $\alpha=1$ ($\beta=1$) refers to row (column) 2, $\alpha=2$ ($\beta=2$) refers to row (column) 1 and $\alpha=3$ ($\beta=3$) refers to row (column) 3. This particular order will lead to simplification of the notation. The integral equation (B1) now becomes

$$T_{\alpha\beta}(\mathbf{q},\mathbf{q}')=(2\pi)^3\delta(\mathbf{q}-\mathbf{q}')\delta_{\alpha\beta}$$
$$+\sum_{\gamma=1}^{3}\int(2\pi)^{-3}d\mathbf{q}''K_{\alpha\gamma}(\mathbf{q},\mathbf{q}'')\tau^{\gamma}(q'')T_{\gamma\beta}(\mathbf{q}'',\mathbf{q}'), \quad \text{(B8)}$$

where $\tau^{\gamma}(q'')$ is given in Sec. II.A (where the numbering of the rows and columns is normal). The matrix $T_{\alpha\beta}(\mathbf{q},\mathbf{q}')$ is defined in terms of the left member of Eq. (B6) in the same way that $K_{\alpha\beta}(\mathbf{q},\mathbf{q}')$ has been defined in terms of the kernel of that equation. Equation (B5) now becomes

$$T=2v_1(k,I)T_{\alpha\beta}(\mathbf{q},\mathbf{q}')\tau^{\beta}(q')v_1(k',I'). \quad \text{(B9)}$$

Combining this with Eq. (1), the matrix element M_{ab} becomes

$$M_{ab}=2(2\pi)^{-12}\sum_{\alpha,\beta\neq 2}\int d\mathbf{q}d\mathbf{k}d\mathbf{q}'d\mathbf{k}'\phi_a(\mathbf{q},\mathbf{k})U^{21}(0,I(\alpha))$$
$$\times v_1(k,I(\alpha))T_{\alpha\beta}(\mathbf{q},\mathbf{q}')\tau^{\beta}(q')v_1(k',I(\beta))$$
$$\times U^{12}(0,I(\beta))\phi_b(\mathbf{q}',\mathbf{k}'), \quad \text{(B10)}$$

where $\phi_a(\mathbf{q},\mathbf{k})$ is the product of the deuteron wave function and a plane-wave kaon wave function, both written in the natural coordinate system number 1. Here the isospin $I(\alpha)$ equals 1 if $\alpha=3$ and equals 0 if $\alpha=1$. The factor $(2\pi)^{-3}\int\phi_a(\mathbf{q},\mathbf{k})v_1(k,I(\alpha))d\mathbf{k}\times U^{21}(0,I(\alpha))$ is easily evaluated due to the δ function representing the plane-wave kaon and is found to be

$$v_1((m_2/\mathfrak{M}_1)\mathbf{q}+\mathbf{q}_a, I(\alpha))\phi_D((m_1/\mathfrak{M}_2)\mathbf{q}_a+\mathbf{q})$$
$$\times U^{21}(0,I(\alpha)), \quad \text{(B11)}$$

where $\phi_D(\mathbf{k})$ is the deuteron wave function written in its natural coordinate system (i.e., No. 2) and $\mathbf{q}_a$ is the initial momentum of the kaon in the c.m. system. This entire factor (B11) is denoted by $\Phi_{\alpha 2}(q)$.

Making a partial wave analysis of Eqs. (B8) and (B10) leads to the equations

$$M_{ab}=\sum_l(2l+1)\eta_l P_l(\hat{q}_a\cdot\hat{q}_b), \quad \text{(B12)}$$

$$\eta_l=\sum_{\alpha,\beta\neq 2}\int_0^{\infty}q^2dq\int_0^{\infty}q'^2dq'(2\pi)^{-4}\Phi_{l\alpha 2}(q)$$
$$\times[T_{l\alpha\beta}(q,q')\tau^{\beta}(q')]\Phi_{lb2}(q'), \quad \text{(B13)}$$

where $\Phi_{l\alpha 2}(q)$ is defined by

$$\Phi_{l\alpha 2}(q)=(2\pi)^{-1}\int P_l(\hat{q}\cdot\hat{q}_a)\Phi_{\alpha 2}(\mathbf{q})d\Omega_q, \quad \text{(B14)}$$

and where $T_{l\alpha\beta}(q,q')$ is defined by

$$T_{l\alpha\beta}(q,q')=(2\pi)^{-1}\int P_l(\hat{q}\cdot\hat{q}')T_{\alpha\beta}(\mathbf{q},\mathbf{q}')d\Omega_q. \quad \text{(B15)}$$

The factor in square brackets in Eq. (B13) can be rewritten as

$$T_{l\alpha\beta}(q,q')\tau^{\beta}(q')=\tau^{\beta}(q')(2\pi/q)^2\delta(q-q')$$
$$+\tau^{\alpha}(q)R_{l\alpha b}(q,q')\tau^{\beta}(q'), \quad \text{(B16)}$$

where

$$R_{l\alpha\beta}(q,q')=K_{l\alpha\beta}(q,q')$$
$$+\sum_{\gamma}\int_0^{\infty}\frac{(q'')^2dq''}{(2\pi)^2}K_{l\alpha\gamma}(q,q'')\tau^{\gamma}(q'')R_{l\gamma\beta}(q'',q'). \quad \text{(45')}$$

Equation (B16) together with (B13) immediately yields Eqs. (36) and (37). Equation (B12) thus becomes Eq. (35), while Eq. (45') is identical with Eq. (45). Derivation of Eq. (38) is straightforward from the definition Eq. (B14), after noting that the deuteron wave function for the Yamaguchi potential is just

$$\phi_D(k)=N(\alpha_2^2+k^2)^{-1}(\beta_2^2+k^2)^{-1},$$

where

$$N^2=8\pi\alpha_2\beta_2(\alpha_2+\beta_2)^3,$$

and

$$\alpha_2^2=mB_2.$$

where m is the nucleon mass and B_2 is the deuteron binding energy. Note that C_2 is defined equal to zero in Eq. (44), so that the summations in Eqs. (36) and (37) do not need to be restricted. The derivation of Eq. (46) is entirely similar to the derivation of Eq. (38). The matrix $W_{\alpha\beta}$ includes the appropriate elements of $U^{ik}(I,K)$ as given at the end of Appendix A together with the occasional square roots of 2 appearing in (B7).